The Journal of Neuroscience, March 1994, 14(3): 1332–1338

Muscarine Hyperpolarizes a Subpopulation of Neurons by Activating an M_2 Muscarinic Receptor in Rat Nucleus Raphe Magnus *in vitro*

Z. Z. Pan and J. T. Williams

Vollum Institute, Oregon Health Sciences University, Portland, Oregon 97201

It has been shown previously that the muscarinic cholinergic system in the nucleus raphe magnus (NRM) is involved in the modulation of nociception. In this study, we examined the direct actions of muscarine on the NRM neurons in a slice preparation. Muscarine (1–30 μM) produced a dose-dependent hyperpolarization in a subpopulation of the NRM cells that contain 5-hydroxytryptamine (5-HT). In voltage clamp, the muscarine-induced outward current reversed polarity at the potassium equilibrium potential and was characterized by strong inward rectification. The reversal potential was dependent on external potassium concentration, suggesting that the hyperpolarization induced by muscarine was mediated through an increase in an inwardly rectifying potassium conductance. 5-HT also hyperpolarized these cells by increasing the same inwardly rectifying potassium conductance. The concentration–response curve for muscarine (EC_{50} = 2.7 μM) was shifted in a parallel manner to the right by increasing concentrations of pirenzepine (300 nM to 3 μM) and methoctramine (50–200 nM). Schild analysis revealed that the equilibrium dissociation constant (K_d) was 230 nM for pirenzepine and was estimated to be less than 30 nM for methoctramine. These results indicate that the muscarinic receptor mediating the muscarine activation of the potassium conductance in these cells is of the M_2 subtype. The present results suggest an inhibitory cholinergic postsynaptic modulation on the activity of a subpopulation of serotonergic neurons that are involved in antinociceptive function in the NRM.

[Key words: muscarine, M_2 muscarinic receptor, inwardly rectifying potassium conductance, pirenzepine, methoctramine, nucleus raphe magnus]

Neurons in the nucleus raphe magnus (NRM) are involved in the descending modulation of nociceptive processing from supraspinal levels (Basbaum and Fields, 1984). Functionally, there are different groups of putative pain-modulating neurons in the NRM and modulation of the activity in these neurons by opioids and other neurotransmitters results in a significant change in pain threshold (Fields et al., 1983, 1991). Among those neurotransmitters is ACh. Cholinergic (AChE- or ChAT-positive) cells have been identified within the NRM in previous anatomical studies (Bowker et al., 1983; Jones et al., 1986; Sherriff et al., 1991). The NRM receives cholinergic afferents originating from the cells in the pedunculopontine tegmental nucleus (Rye et al., 1988). Behavioral studies have shown that local applications of both muscarinic receptor agonists and antagonists into the NRM cause antinociception (Brodie and Proudfit, 1986; Iwamoto, 1991). In previous *in vivo* studies, iontophoretic application of ACh has been reported to induce an inhibition or excitation in the spontaneous activity of different groups of the NRM cells (Behbehani, 1982; Wessendorf and Anderson, 1983; Willcockson et al., 1983; Hentall et al., 1993). Neither the cellular mechanism underlying the actions of these cholinergic agents on NRM neurons nor the muscarinic receptor subtypes that mediate the cholinergic actions is known.

The actions of ACh acting at muscarinic receptors in the CNS include a depolarization resulting from a reduction in a potassium conductance (Brown and Adams, 1980; Madison et al., 1987; Uchimura and North, 1990) and a hyperpolarization as a result of an increase in a potassium conductance (Egan and North, 1986; McCormick and Prince, 1987; McCormick and Pape, 1988; Gerber et al., 1991). Muscarinic cholinergic receptors consist of a heterogeneous family of five different subtypes (m1–m5) that have been cloned from rats (Kubo et al., 1986; Bonner et al., 1987, 1988). The m1–m3 receptors correspond most closely to the pharmacologically defined M_1–M_3 receptors (Kubo et al., 1986; Brann et al., 1988; Maeda et al., 1988; Buckley et al., 1989). The m1, m3, and m5 receptors are functionally coupled primarily to the stimulation of inositol phosphate metabolism through a pertussis toxin–insensitive G-protein, while the m2 and m4 receptors are associated mainly with an inhibition of cAMP production through a pertussis toxin–sensitive G-protein (Bonner et al., 1988; Fukuda et al., 1988; Peralta et al., 1988; Wess et al., 1990; Lai et al., 1991). In rat brainstem, the presence of all five receptor subtypes or their mRNAs has been reported (Buckley et al., 1988; Ehlert and Tran, 1990; Levey et al., 1991; Li et al., 1991; Zubieta and Frey, 1993).

In this study, we examined the direct actions of muscarine on the neurons in the NRM in a slice preparation and then identified the ionic mechanism and the receptor subtype involved in the muscarine-induced hyperpolarization observed in a subpopulation of neurons in the NRM.

Preliminary results of this study have been presented as an abstract (Pan and Williams, 1991).

Materials and Methods

Intracellular recordings were made from NRM cells in brain slices from adult Wistar rats. The methods employed were similar to those published previously (Pan et al., 1990). Briefly, brain slices (300 μm thick)

Received Mar. 31, 1993; revised Aug. 4, 1993; accepted Aug. 19, 1993.

We thank Drs. D. Cameron and M. Kelly for comments on the manuscript. This work was supported by NIH Grants DA04523 and DA00141.

Correspondence should be addressed to J. T. Williams, Vollum Institute, Oregon Health Sciences University, 3181 SW Sam Jackson Park Road, Portland, OR 97201.

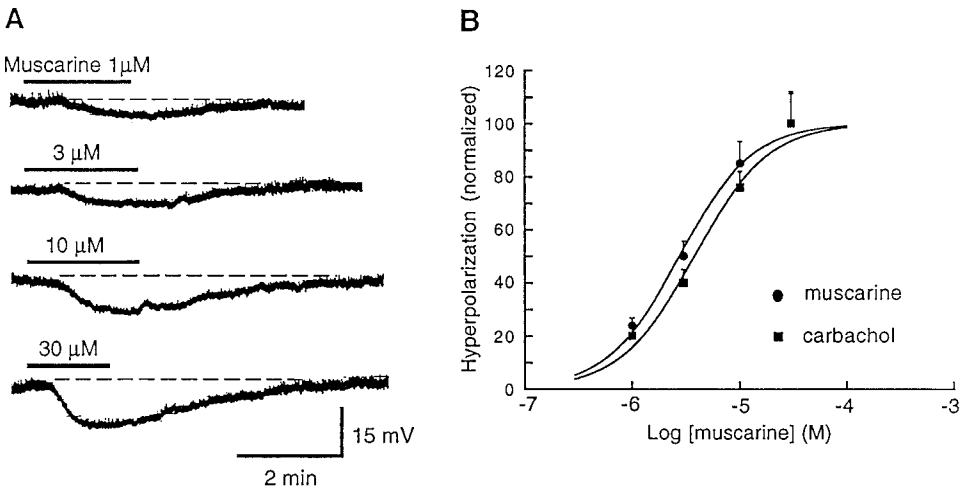

Figure 1. Hyperpolarization induced by muscarinic receptor agonists in neurons in the NRM. *A*, Membrane potential recordings of an NRM cell that was hyperpolarized by increasing concentrations of muscarine. *B*, Dose–response curves for the hyperpolarization induced by muscarine (EC_{50} = 2.7 μM, n = 8) and by carbachol (EC_{50} = 3.8 μM, n = 7). Data points are expressed as a percentage of the maximum hyperpolarization by 30 μM muscarine (9.8 ± 1.1 mV) and by 30 μM carbachol (9.4 ± 1.1 mV), respectively. Error bars are SE of the mean.

were cut in a vibratome in cold (4°C) physiological saline. Two or three coronal slices were taken from the level of the facial nerve in each brain. A single slice was submerged in a tissue bath through which flowed physiological saline (1.5 ml/min) at 37°C. The content of physiological saline solution was (in mM) NaCl, 126; KCl, 2.5; NaH_2PO_4, 1.2; $MgCl_2$, 1.2; CaCl, 2.4; glucose, 11; $NaHCO_3$, 25; gassed with 95% O_2, 5% CO_2 at 37°C.

The NRM was recognized in the slice as a triangular area in the midline just above the pyramidal tracts. Neurons were penetrated with glass microelectrodes filled with potassium chloride (2 M) having resistances of 40–70 MΩ. Membrane currents were recorded with a single-electrode voltage-clamp amplifier (Axoclamp 2A) using switching frequencies between 3 and 6 kHz. The settling time of the clamp following a 10 mV step was typically 3–5 msec. Steady state current–voltage (*I–V*) plots were constructed directly on an x,y-plotter using a slow depolarizing ramp potential. The speed of the ramp (1 mV/sec) was sufficiently slow to give the same current as that measured at the termination of a 2 sec voltage step.

Drugs were applied by superfusion. The following drugs and salts were used: muscarine (Sigma), carbachol (Sigma), pirenzepine (PZP; Research Biochemical Inc.), methoctramine (Research Biochemicals Inc.), 5-hydroxytryptamine (5-HT; Sigma), 5-carboxamidotryptamine (5-CT; Glaxo), $BaCl_2$ (Sigma), tetrodotoxin (TTX; Sigma). Dose–response data were fitted by logistic equation and the EC_{50} was then determined. Schild analysis was carried out by determining the dose ratios at the EC_{50} values in the absence and presence of the antagonist (Schild, 1949). Numerical data are presented as means ± SE of the means and compared using an unpaired, two-tailed Student's t test.

Results

In a previous study, two groups of cells in the NRM have been described: primary and secondary (Pan et al., 1990). Primary cells have action potential duration of >1 msec and are 5-HT containing (>90%, Pan et al., 1993); opioids do not affect the resting membrane potential but inhibit the GABA synaptic potential in primary cells. Secondary cells have shorter action potential duration (<1 msec) and are hyperpolarized by opioids. Muscarinic agonists were tested on a total of 148 cells: 73 cells were hyperpolarized, 21 cells were depolarized, and 54 cells were not affected. TTX (1 μM) did not change the muscarine-induced depolarization or hyperpolarization in all cells tested (n = 24).

Muscarine hyperpolarized a subgroup of primary cells

Of the 148 cells, 98 were unequivocally identified (74 primary, 24 secondary). In the primary cell group, 41 cells were hyperpolarized by muscarine (55%; Fig. 1*A*), no depolarizations were observed, and the other 33 primary cells were not affected. The muscarine-induced hyperpolarization had a threshold at 1 μM and a maximum hyperpolarization of 9.8 ± 1.1 mV (n = 8) at 30 μM. The EC_{50} was 2.7 μM (Fig. 1*B*). Carbachol, a muscarinic receptor agonist, also hyperpolarized these cells in a dose-dependent manner over a similar concentration range (1–30 μM; Fig. 1*B*), inducing a maximum hyperpolarization of 9.4 ± 1.1 mV (n = 7) at 30 μM and having an EC_{50} of 3.8 μM.

In 21 of 148 cells (14%), muscarine (10 μM) induced a depolarization of 4.8 ± 0.6 mV (n = 21), which often resulted in the firing of repetitive action potentials. The muscarine-induced depolarization was observed almost exclusively in secondary cells.

Muscarine activated an inwardly rectifying potassium conductance

In voltage clamp, muscarine produced an outward current at the resting membrane potential associated with an increase in membrane conductance (n = 24; Fig. 2*A*). At more negative potentials than the resting potential, the muscarine-induced current declined in amplitude and reversed polarity. The averaged reversal potential of the muscarine-induced current was −103 ± 2 mV (n = 17) in normal concentration of external potassium (2.5 mM). When the potassium concentration in the perfusing solution was increased to 6.5 mM and 10.5 mM, the reversal potential was shifted to −78 ± 2 mV (n = 11) and −66 ± 2 mV (n = 7), respectively (Fig. 2*B*), giving a Nernst slope of −59.5 (Fig. 2*C*). This suggested a primary involvement of a potassium conductance.

The muscarine-induced current exhibited inward rectification that was more obvious in higher concentrations of external potassium (Fig. 3*A*). In 6.5 mM external potassium, the slope conductance of the muscarine-induced current measured between −50 and −60 mV was 1.0 ± 0.2 nS and 5.2 ± 1.0 nS between −100 and −110 mV (n = 10). Barium (30 μM) blocked the inwardly rectifying part of the muscarine current leaving a small, linear current (Fig. 3*A*).

Muscarine and 5-HT hyperpolarized the cell by increasing the same inwardly rectifying potassium conductance

Many cells in the NRM were hyperpolarized by 5-HT (10 or 30 μM). The currents induced by 5-HT in voltage clamp had the same inward rectification and barium sensitivity as that induced by muscarine. The slope conductance of the 5-HT–induced current was 1.2 ± 0.1 nS between −50 and −60 mV

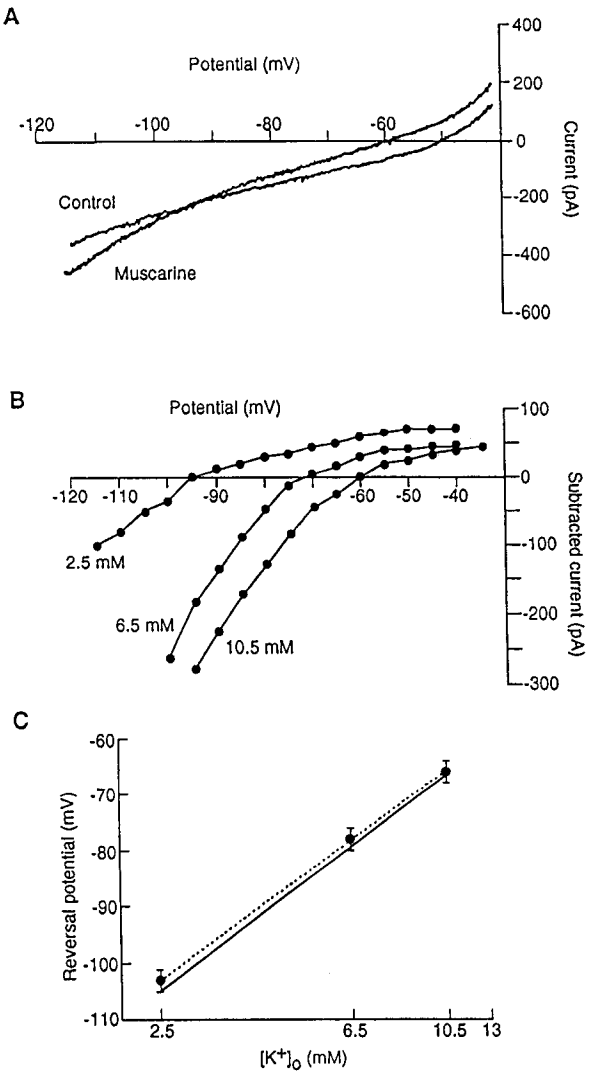

Figure 2. Muscarine-induced hyperpolarization is mediated through an increase in an inwardly rectifying potassium conductance. *A*, Steady state current–voltage plots in the absence and presence of muscarine (10 μM). The reversal potential is −94 mV. *B*, The current–voltage plots of the muscarine-induced current in three different external potassium concentrations from the same cell as in *A*. The muscarine-induced currents were determined by manual subtraction of the current in control from that in muscarine at 5 mV intervals. *C*, Dependence of the reversal potential of the muscarine current on the external potassium concentrations. The *dotted line* is the fit to the data points (means of 7–17 experiments, slope = −59.5). The *solid line* was determined by the Nernst equation where the internal potassium concentration was fixed at 135 mM.

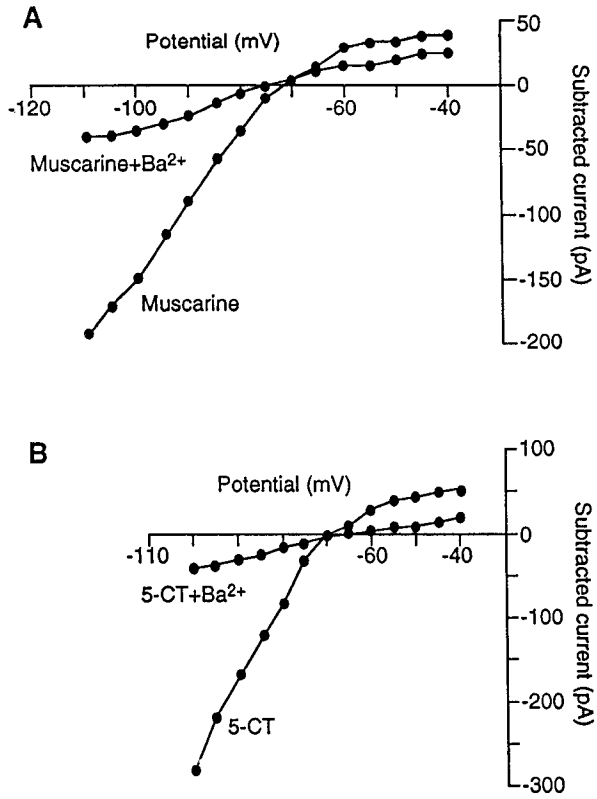

Figure 3. Inward rectification of the currents induced by muscarine and by 5-CT. The experiment was carried out in 6.5 mM external potassium concentration. *A*, The current–voltage plots of muscarine-induced currents in control and in the presence of $BaCl_2$ (30 μM), showing that the muscarine-induced current rectified inwardly and that barium blocked the inward rectification of the muscarine current. *B*, Subtracted currents induced by 5-CT (300 nM), a 5-HT_1 receptor agonist, in control and in $BaCl_2$ (30 μM) from another cell. Note the similarities in inward rectification and barium sensitivity of the 5-CT current to the muscarine current shown in *A*.

and 8.4 ± 0.8 nS between −100 and −110 mV. $BaCl_2$ (30 μM) abolished the inward rectification of the current induced by the 5-HT_1 receptor agonist 5-CT (300 nM; Fig. 3*B*). Then the effect of muscarine was tested in the cells that were hyperpolarized by 5-HT. Out of 102 cells that were hyperpolarized by 5-HT, 58 cells (57%) were hyperpolarized by muscarine (Fig. 4*A*). The hyperpolarizations induced by muscarine and by 5-HT were not additive. The membrane potential of other 5-HT–responding cells was either not affected (n = 41, 40%) or depolarized (n = 3, 3%) by muscarine (10 or 30 μM).

In voltage clamp, muscarine (30 μM) caused no more current in cells that were already treated with 5-HT (30 μM) or 5-CT (300 nM; n = 4; Fig. 4*B*). These results suggest that the same inwardly rectifying potassium conductance is involved in the muscarine- and 5-HT–induced hyperpolarization in these NRM cells.

Muscarine-induced hyperpolarization is mediated through an M_2 receptor subtype

To identify the receptor subtype involved in the muscarine action, the concentration–response relationship for muscarine was constructed in the absence and presence of different concentrations of the muscarinic receptor antagonists PZP and methoctramine.

The control dose–response curve for muscarine (EC_{50} = 2.7 μM) was shifted to the right by increasing concentrations of PZP (Fig. 5*A*). These shifts were parallel and the same maximum effect was maintained, indicating a competitive antagonism. The EC_{50} for muscarine was 6.0 μM, 15.4 μM, and 44.3 μM in 300 nM (n = 4), 1 μM (n = 4), and 3 μM PZP (n = 3), respectively. The K_d for PZP for the receptor subtype mediating the muscarine response was estimated using Schild analysis. Dose ratios were determined by EC_{50} values in different concentrations of PZP divided by the EC_{50} in control. We chose to use EC_{50} for the Schild analysis because the value was within the straight portion of parallel dose–response curves. The resulting Schild plot (Fig. 5*B*) was linear and the best-fitted line through the data points

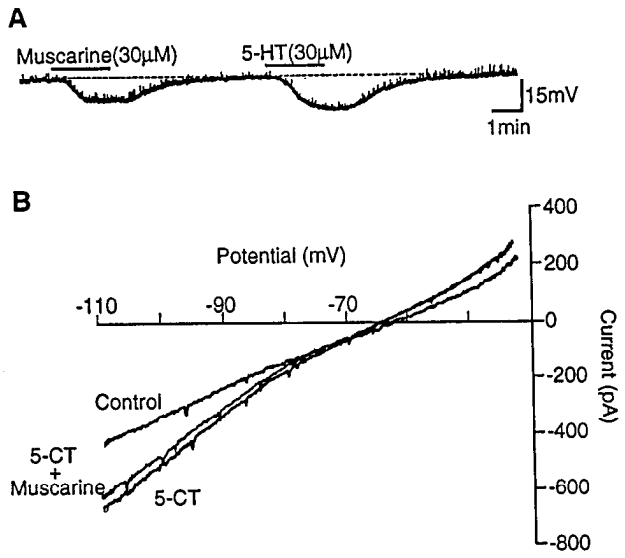

Figure 4. Muscarine and 5-HT hyperpolarize the cell by increasing the same inwardly rectifying potassium conductance. *A*, A membrane potential recording of a cell that was hyperpolarized by both muscarine and 5-HT. *B*, Steady state current–voltage plots in control, in the presence of 5-CT, and in 5-CT (300 nM) plus muscarine (10 μM). In the presence of 5-CT, addition of muscarine caused no more current.

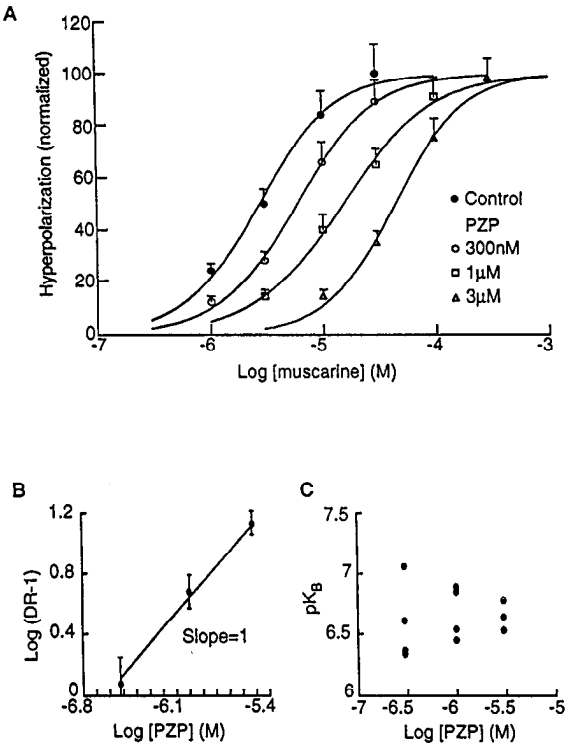

Figure 5. Competitive antagonism of the muscarine-induced hyperpolarization by increasing concentrations of PZP. *A*, Dose–response curves for muscarine in control (EC_{50} = 2.7 μM, n = 8) and in the presence of 300 nM (EC_{50} = 6.0 μM, n = 4), 1 μM (EC_{50} = 15.4 μM, n = 4), and 3 μM PZP (EC_{50} = 44.3 μM, n = 3). Data points are presented as a percentage of the maximum hyperpolarization (9.8 ± 1.1 mV) in control. *B*, Schild regression to PZP from data shown in *A*. Slope = 1.0 (95% confidence limits, 0.8–1.2). pK_B = 6.64 (range of 6.49–6.79). Dose ratios were determined as described in Materials and Methods. Data points are the means at each PZP concentration. *C*, Regression of pK_B estimates calculated from individual PZP concentration and the resulting dose ratio on the corresponding PZP concentration. No significant regression is obtained (t = 0.4, df = 9).

had a slope of 1.05 that is not significantly different from unity. pK_B was calculated for each concentration of PZP and the corresponding dose ratio (DR) according to the equation: $pK_{Bi} = \log(DR - 1)_i - \log[PZP]_i$. The mean pK_B calculated from each pK_{Bi} (n = 11) was 6.64 ± 0.07 (95% confidence limits, 6.49–6.79) and the K_d for PZP was 230 nM (162–324 nM). Regression of calculated pK_B estimates on the corresponding concentrations of PZP is shown in Figure 5*C*. No significant regression was obtained (t = 0.4, df = 9), indicating that the estimated pK_B values (thus the K_d for PZP) were independent of the antagonist concentration.

The dose–response curve for muscarine was also shifted to the right with the same maximum effect by increasing concentrations of methoctramine (Fig. 6*A*). The EC_{50} for muscarine was 10.7 μM and 23.1 μM in 50 nM (n = 5) and 100 nM (n = 4) methoctramine, respectively. In 200 nM methoctramine (n = 3), the EC_{50} was 83.9 μM, 31-fold larger than that in control. The Schild plot shown in Figure 6*B* had a best-fitted line (x-intercept = −7.56) with a slope of 1.67. This value was significantly different from unity, possibly indicating nonequilibrium steady states in drug–receptor interactions at the lower antagonist concentrations (see Discussion). The K_d value calculated from the dose ratio (31-fold) at 200 nM methoctramine was then estimated to be 7 nM, according to the equation K_d = [antagonist]/(DR − 1) (Kachur et al., 1990).

Discussion

The muscarinic receptor subtype involved

The coupling of muscarinic receptor activation to a potassium conductance increase in the CNS was first reported by Egan and North (1986) in rat parabrachial neurons. Involvement of an M_2 (previous definition) subtype was suggested based on the lower affinity of the receptor for PZP (K_d = 600 nM) versus the higher-affinity PZP sites (M_1) (Hammer et al., 1980). Further development of muscarinic receptor antagonists has resulted in the current recognition of three pharmacologically defined subtypes with the M_2 further divided into M_2 (previously defined cardiac M_2) and M_3 (previous glandular M_2) (Bonner, 1989). In addition, five different muscarinic receptors have been cloned and radioligand binding studies have demonstrated that none of the antagonists has fivefold or higher affinity for one subtype over another (Buckley et al., 1989). In the present study, PZP and methoctramine were used to determine the receptor subtype involved because of their higher ability to discriminate by affinity the M_1 and M_2 subtypes, respectively, from other subtypes (Buckley et al., 1989).

Previously, in both radioligand binding studies (Akiba et al., 1988; Lai et al., 1988; Buckley et al., 1989; Lazareno and Roberts, 1989; Mei et al., 1989; Dorje et al., 1991) and functional studies (Lai et al., 1988; Lazareno and Roberts, 1989; McKinney et al., 1989a,b; Kachur et al., 1990; Sugita et al., 1991), PZP has been shown to have the following rank order of potency: M_1 (K_d range, 3–33 nM) > m4 (37–120 nM, binding studies) > m5 (89–170 nM, binding studies) > M_3 (102–186 nM) > M_2 (219–906 nM). Our results indicate that PZP had a K_d of 230 nM for the receptor mediating the muscarine response, suggesting that the receptor is a non-M_1 subtype and the PZP K_d falls within the previously reported K_d range for the M_2 subtype.

The rank order of potency for methoctramine has been shown

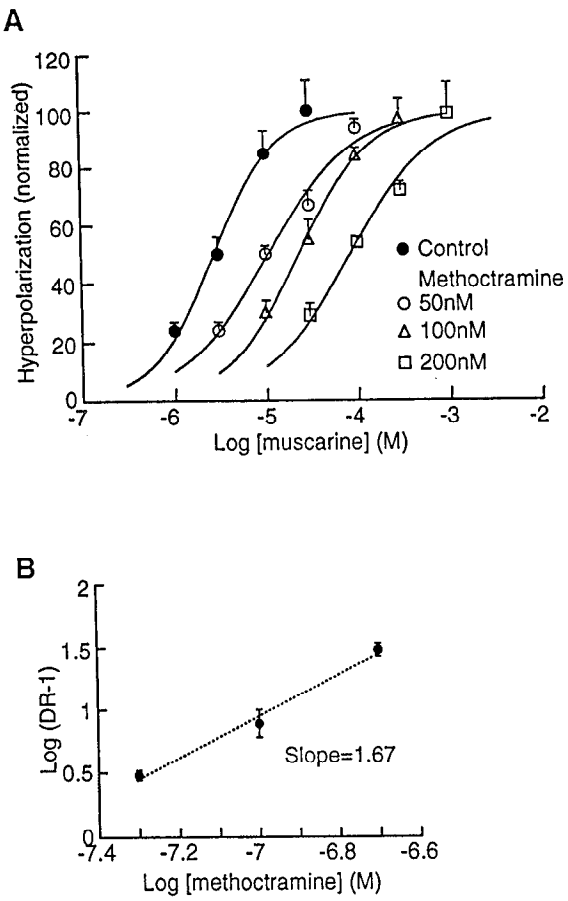

Figure 6. Competitive antagonism of the muscarine-induced hyperpolarization by increasing concentrations of methoctramine. *A*, Dose–response curves for muscarine in control (EC_{50} = 2.7 μM, n = 8) and in the presence of 50 nM (EC_{50} = 10.7 μM, n = 5), 100 nM (EC_{50} = 23.1 μM, n = 4), and 200 nM methoctramine (EC_{50} = 83.9 μM, n = 3). Data points represent the percentage of the maximum hyperpolarization in control. *B*, Schild regression to methoctramine from data shown in *A*. *Solid circles* are means at each methoctramine concentration. The *dashed line* is the best-fitted line through the data points (r = 0.995). Slope = 1.67; x-intercept = −7.56.

as follows: M_2 (K_d range, 4–47 nM) > M_1 (16–50 nM) > m4 (32–40 nM) > m5 (57–135 nM) > M_3 (118–776 nM) from both binding studies (Buckley et al., 1989; Lazareno and Roberts, 1989; Wess et al., 1990; Dorje et al., 1991) and functional studies (Melchiorre et al., 1987; Lazareno and Roberts, 1989; McKinney et al., 1989b; Kachur et al., 1990; Sugita et al., 1991). Among the selective M_2 antagonists, methoctramine is comparatively the best in discriminating M_2 from the other three subtypes with the M_1 subtype excluded (Bonner, 1989). In the present study, no reliable K_d value for methoctramine could be obtained as the slope of the Schild plot was significantly greater than unity. This most likely resulted from nonequilibrium steady states in the drug–receptor interactions at the lower antagonist concentrations, due to an inadequate period of time (20 min in this study) for equilibrium to be achieved. This would result in an underestimate of the dose ratio at the lower antagonist concentrations and a steeper Schild regression slope. If this is the case, the equilibrium conditions could be obtained by increasing the interaction time at lower concentrations of the antagonist (practically difficult in this study). The K_d estimate with a slope of unity would then be smaller than the value indicated by the x-intercept of a fitted line with the slope greater than unity (Kenakin, 1987). In our case, the actual pK_B value was probably less than −7.56 as indicated by the x-intercept of best-fitted line through the data points (thus K_d < 28 nM). As an estimate, the K_d calculated from the dose ratio (31-fold) at 200 nM methoctramine was 7 nM. Therefore, the K_d for methoctramine appears to be <30 nM, which is consistent with the previously described methoctramine K_d range for the M_2 subtype.

Taken together, it seems reasonable to conclude that the muscarinic receptor mediating the hyperpolarization in these NRM cells is of the M_2 subtype. This is in agreement with previous anatomical studies, where a relatively high density of M_2 and low density of M_1 and M_3 receptors (Buckley et al., 1988; Ehlert and Tran, 1990; Levey et al., 1991; Li et al., 1991; Zubieta and Frey, 1993) were found in rat brainstem structures including the NRM (Quirion et al., 1989). Only low levels of m4 and m5 receptor proteins were detected in the rat brainstem area (Levey et al., 1991; Yasuda et al., 1993).

The inwardly rectifying potassium conductance

We have shown that the muscarine-induced hyperpolarization in these NRM neurons was mediated through an increase in a barium-sensitive, inwardly rectifying potassium conductance. The muscarinic receptor activation of the potassium conductance originally reported in the CNS parabrachial neurons (Egan and North, 1986) was linearly dependent on the membrane potential. Recently, Gerber et al. (1991) characterized an inwardly rectifying potassium conductance activated by muscarinic agonists in rat pontine reticular formation neurons and the involvement of a non-M_1 subtype was suggested. The potassium conductance in that study was similar in both the membrane potential dependence (inward rectification) and barium sensitivity to that described here. We have also shown that both muscarine and 5-HT hyperpolarized a subgroup of NRM cells through an increase in a similar inwardly rectifying potassium conductance. The reversal potentials of both 5-HT and muscarinic currents were at the predicted potassium equilibrium potential, indicating that voltage control was sufficient for each and suggesting that the currents arose from areas of the cell that were electrotonically similar. In addition, the currents induced by muscarine and by 5-CT were not additive. We and others have used this approach to suggest that different agonists acting on separate receptors activate a common inwardly rectifying potassium conductance (North and Williams, 1985; Andrade et al., 1986; Christie and North, 1988).

Functional considerations

The results reported here are consistent with previous *in vivo* studies where iontophoretic application of ACh into the NRM inhibited the spontaneous activity in the majority of the cells (Wessendorf and Anderson, 1983; Hentall et al., 1993). In addition, a more consistent inhibition was found specifically in raphe-spinal serotonergic cells (Wessendorf and Anderson, 1983). Other studies, however, have reported excitation of most cells in the NRM in response to iontophoretic ACh (Behbehani, 1982; Willcockson et al., 1983). This discrepancy may largely be attributed to the use of ACh that can act on both muscarinic and nicotinic receptors. Both receptor types are thought to be involved in modulation of the cellular activity and of antinociceptive function of the NRM (Iwamoto, 1991).

Generally, the activation of the cells, particularly the raphe-

spinal projection cells, in the NRM produces antinociception through descending inhibition (Basbaum and Fields, 1984). A recent behavioral study has shown that local injection of methoctramine into the NRM produced a strong antinociceptive response in rats (Iwamoto, 1991). This implies the possibility of a tonic inhibitory muscarinic modulation of the NRM neurons responsible for the descending inhibition. In an earlier report, local application of the muscarinic receptor agonist carbachol into the NRM also induced antinociception. However, this effect did not appear to be mediated by serotonergic neurons in the NRM (Brodie and Proudfit, 1986). The present results implicate an inhibitory cholinergic postsynaptic modulation on some of the serotonergic neurons in the NRM. These same neurons could presumably be activated by opioids through GABA-mediated disinhibition and may contribute to the descending modulation of sensory inputs (Pan et al., 1990).

References

Akiba I, Kubo T, Maeda A, Bujo H, Naka J, Mishina M, Numa S (1988) Primary structure of porcine muscarinic acetylcholine receptor III and antagonist binding studies. FEBS Lett 235:257–261.

Andrade R, Malenka RC, Nicoll RA (1986) A G protein couples serotonin and $GABA_b$ receptors to the same channel in hippocampus. Science 234:1261–1265.

Basbaum AI, Fields HL (1984) Endogenous pain control systems: brainstem spinal pathways and endorphin circuitry. Annu Rev Neurosci 7:309–338.

Behbehani MM (1982) The role of acetylcholine in the function of the nucleus raphe magnus and in the interaction of this nucleus with the periaqueductal gray. Brain Res 252:299–307.

Bonner TI (1989) New subtypes of muscarinic acetylcholine receptors. Trends Pharmacol Sci 10:11–15.

Bonner TI, Buckley NJ, Young AC, Brann MR (1987) Identification of a family of muscarinic acetylcholine receptor genes. Science 237: 527–532.

Bonner TI, Young AC, Brann MR, Buckley NJ (1988) Cloning and expression of the human and rat m5 muscarinic acetylcholine receptor genes. Neuron 1:403–410.

Bowker RM, Westlund KN, Sullivan MC, Wilber JF, Coulter JD (1983) Descending serotonergic, peptidergic and cholinergic pathways from the raphe nuclei: a multiple transmitter complex. Brain Res 1983:33–48.

Brann MR, Buckley NJ, Bonner TI (1988) The striatum and cerebral cortex express different muscarinic receptor mRNAs. FEBS Lett 230: 90–94.

Brodie MS, Proudfit HK (1986) Antinociception induced by injection of carbachol into the nucleus raphe magnus in rats: alteration by intrathecal injection of monoaminergic antagonists. Brain Res 371: 70–79.

Brown DA, Adams PR (1980) Muscarinic suppression of a novel voltage-sensitive K^+ current in a vertebrate neuron. Nature 283:673–676.

Buckley NJ, Bonner TI, Brann MR (1988) Localization of a family of muscarinic receptor mRNAs in rat brain. J Neurosci 8:4646–4652.

Buckley NJ, Bonner TI, Buckley CM, Brann MR (1989) Antagonist binding properties of five cloned muscarinic receptors expressed in CHO-K1 cells. Mol Pharmacol 35:469–476.

Christie MJ, North RA (1988) Agonists at μ-opioid, M2-muscarinic and $GABA_b$-receptors increase the same potassium conductance in rat lateral parabrachial neurones. Br J Pharmacol 95:896–902.

Dorje F, Wess J, Lambrecht G, Tacke R, Mutschler E, Brann MR (1991) Antagonist binding profiles of five cloned human muscarinic receptor subtypes. J Pharmacol Exp Ther 256:727–733.

Egan TM, North RA (1986) Acetylcholine hyperpolarizes central neurons by acting on an M_2 muscarinic receptor. Nature 319:405–407.

Ehlert FJ, Tran LLP (1990) Regional distribution of M1, M2 and non-M1, non-M2 subtypes of muscarinic binding sites in rat brain. J Pharmacol Exp Ther 255:1148–1157.

Fields HL, Vanegas H, Hentall ID, Zoeman G (1983) Evidence that disinhibition of brain stem neurons contributes to morphine analgesia. Nature 306:684–686.

Fields HL, Heinricher MM, Mason P (1991) Neurotransmitters in nociceptive modulatory circuits. Annu Rev Neurosci 14:219–245.

Fukuda K, Higashida T, Kubo T, Maeda A, Akiba I, Bujo H, Mishina M, Numa S (1988) Selective coupling with K^+ currents of muscarinic acetylcholine receptor subtypes in NG108-15 cells. Nature 335: 355–358.

Gerber U, Stevens DR, McCarley RW, Greene RW (1991) Muscarinic agonists activate an inwardly rectifying potassium conductance in medial pontine reticular formation neurons of the rat *in vitro*. J Neurosci 11:3861–3867.

Hammer R, Berrie CP, Birdsall NJM, Burgen ASV, Hulme EC (1980) Pirenzepine distinguishes between different subclass of muscarinic receptors. Nature 283:90–92.

Hentall ID, Andresen MJ, Taguchi K (1993) Serotonergic, cholinergic and nociceptive inhibition or excitation of raphe magnus neurons in barbiturate-anesthetized rats. Neuroscience 52:303–310.

Iwamoto ET (1991) Characterization of the antinociception induced by nicotine in the pedunculopontine tegmental nucleus and the nucleus raphe magnus. J Pharmacol Exp Ther 257:120–133.

Jones BE, Pare M, Beaudet A (1986) Retrograde labeling of neurons in the brain stem following injections of [^{3}H]choline into the rat spinal cord. Neuroscience 18:901–916.

Kachur JF, Sturm BL, Gaginella TS, Noronha-Blob L (1990) Regulation of guinea pig ileal electrolyte transport by M_3-muscarinic acetylcholine receptors *in vitro*. Mol Pharmacol 38:836–840.

Kenakin TP (1987) Pharmacologic analysis of drug–receptor interaction. New York: Raven.

Kubo T, Fukuda K, Mikami A, Maeda A, Takahashi H, Mishina M, Haga T, Haga K, Ichiyama A, Kangawa K, Kojima M, Matsuo H, Hirose T, Numa S (1986) Cloning, sequencing and expression of complementary DNA encoding the muscarinic acetylcholine receptor. Nature 323:411–416.

Lai J, Mei L, Roeske WR, Chung F-Z, Yamamura HI, Venter JC (1988) The cloned murine M_1 muscarinic receptor is associated with the hydrolysis of phosphatidylinositols in transfected murine B82 cells. Life Sci 42:2489–2502.

Lai J, Waite SL, Bloom JW, Yamamura HI, Roeske WR (1991) The m_2 muscarinic acetylcholine receptors are coupled to multiple signaling pathways via pertussis toxin–sensitive guanine nucleotide regulatory proteins. J Pharmacol Exp Ther 258:938–944.

Lazareno S, Roberts FF (1989) Functional and binding studies with muscarinic M_2-subtype selective antagonists. Br J Pharmacol 98:309–317.

Levey AI, Kitt CA, Simonds WF, Price DL, Brann MR (1991) Identification and localization of muscarinic acetylcholine receptor proteins in brain with subtype-specific antibodies. J Neurosci 11:3218–3226.

Li M, Yasuda RP, Wall SJ, Wellsein A, Wolfe BB (1991) Distribution of m2 muscarinic receptors in rat brain using antisera selective for m2 receptors. Mol Pharmacol 40:28–35.

Madison DV, Lancaster B, Nicoll RA (1987) Voltage clamp analysis of cholinergic action in the hippocampus. J Neurosci 7:733–741.

Maeda A, Kubo T, Mishina M, Numa S (1988) Tissue distribution of mRNAs encoding muscarinic acetylcholine receptor subtypes. FEBS Lett 239:339–342.

McCormick DA, Pape H-C (1988) Acetylcholine inhibits identified interneurons in the cat lateral geniculate nucleus. Nature 334:246–248.

McCormick DA, Prince DA (1987) Actions of acetylcholine in the guinea-pig and cat medial and lateral geniculate nuclei, *in vitro*. J Physiol (Lond) 392:147–165.

McKinney M, Anderson D, Vella-Rountree L (1989a) Different agonist–receptor active conformation for rat brain M_1 and M_2 muscarinic receptors that are separately coupled to two biochemical effector systems. Mol Pharmacol 35:39–47.

McKinney M, Anderson D, Forray C, El-Fakahany EE (1989b) Characterization of the striatal M_2 muscarinic receptor mediating inhibition of cyclic AMP using selective antagonists: a comparison with the brainstem M_2 receptor. J Pharmacol Exp Ther 250:565–572.

Mei L, Lai J, Roeske WR, Fraser CM, Venter JC, Yamamura HI (1989) Pharmacological characterization of the M_1 muscarinic receptors expressed in murine fibroblast B82 cells. J Pharmacol Exp Ther 248: 661–670.

Melchiorre M, Angeli P, Lambrecht G, Mutschler E, Picchio MT, Wess (1987) Antimuscarinic action of methoctramine, a new cardioselec-

tive M-2 muscarinic receptor antagonist, alone and in combination with atropine and gallamine. Eur J Pharmacol 144:117–124.

North RA, Williams JT (1985) On the potassium conductance induced by opioids in rat locus coeruleus neurons. J Physiol (Lond) 364:265–280.

Pan ZZ, Williams JT (1991) 5-HT and muscarine hyperpolarize a subpopulation of neurons in rat nucleus raphe magnus *in vitro*. Soc Neurosci Abstr 17:1163.

Pan ZZ, Williams JT, Osborne PB (1990) Opioid actions on single nucleus raphe magnus neurons from rat and guinea-pig *in vitro*. J Physiol (Lond) 427:519–532.

Pan ZZ, Wessendorf MW, Williams JT (1993) Modulation by serotonin of the neurons in rat nucleus raphe magnus *in vitro*. Neuroscience 54:421–429.

Peralta EG, Ashkenazi A, Winsloe JW, Ramachandran J, Capon DJ (1988) Differential regulation of PI hydrolysis and adenylyl cyclase by muscarinic receptor subtypes. Nature 334:434–437.

Quirion R, Araujo D, Regenold W, Boksa P (1989) Characterization and quantitative autoradiographic distribution of [^{3}H]acetylcholine muscarinic receptors in mammalian brain. Apparent labeling of an M_2-like receptor subtype. Neuroscience 29:271–289.

Rye DB, Lee HJ, Saper CB, Wainer BH (1988) Medullary and spinal efferents of the pedunculopontine tegmental nucleus and adjacent mesopontine tegmentum in the rat. J Comp Neurol 269:315–341.

Schild HO (1949) pA_x and competitive drug antagonism. Br J Pharmacol Chemother 4:277–280.

Sherriff FE, Henderson Z, Morrison JFB (1991) Further evidence for the absence of a descending cholinergic projection from the brainstem to the spinal cord in the rat. Neurosci Lett 128:52–56.

Sugita S, Uchimura N, Jiang Z-G, North RA (1991) Distinct muscarinic receptors inhibit release of γ-aminobutyric acid and excitatory amino acids in mammalian brain. Proc Natl Acad Sci 88:2608–2611.

Uchimura N, North RA (1990) Muscarine reduces inwardly rectifying potassium conductance in rat nucleus accumbens neurons. J Physiol (Lond) 422:369–380.

Wess J, Bonner TI, Brann MR (1990) Chimeric m_2/m_3 muscarinic receptors: role of carboxyl terminal receptor domains in selectivity of ligand binding and coupling to phosphoinositide hydrolysis. Mol Pharmacol 38:872–877.

Wessendorf MW, Anderson EG (1983) Single unit studies of identified bulbospinal serotonergic units. Brain Res 279:93–103.

Willcockson WS, Gerhart KD, Cargill CL, Willis WD (1983) Effects of biogenic amines on raphe-spinal tract cells. J Pharmacol Exp Ther 225:637–645.

Yasuda RP, Ciesla W, Flores LR, Wall SJ, Li M, Satkus SA, Weisstein JS, Spagnola BV, Wolfe BB (1993) Development of antisera selective for m4 and m5 muscarinic cholinergic receptors: distribution of m4 and m5 receptors in rat brain. Mol Pharmacol 43:149–157.

Zubieta JK, Frey KA (1993) Autoradiographic mapping of M_3 muscarinic receptors in the rat brain. J Pharmacol Exp Ther 264:415–422.